State-Space versus Input/Output Representations for Cascade Control of Unstable Systems

Louis P. Russo[†] and B. Wayne Bequette*

Howard P. Isermann Department of Chemical Engineering, Rensselaer Polytechnic Institute, Troy, New York 12180-3590

In this paper we show that the traditional methods of analyzing cascade control based on series or parallel input/output relationships should not be used when the primary and secondary processes are coupled through the state-space model and the process is open-loop unstable. The parallels between traditional full state feedback control and cascade control are demonstrated. We use a jacketed CSTR example to show that neither the parallel nor series input/output formulation for cascade control satisfies controllability or stabilizability conditions when the process is open-loop unstable, although these conditions are satisfied by the physical (state-space) model. We also present a cascade control design procedure which incorporates the "inner"-loop controller in the "outer"-loop design.

1. Introduction

1.1. Motivation. A common control configuration in chemical processes is cascade control; a CSTR application is shown in Figure 1. In this cascade control configuration there is one manipulated variable (the cooling jacket flowrate) and more than one measurement (the reactor temperature and cooling jacket temperature); cascade control is a single-input multiple-output (SIMO) feedback control strategy. The major benefit of cascade control is that action is taken to reject inner-loop disturbances before they effect the outer loop. Therefore, the inner loop of the cascade control strategy is generally tuned very tightly in order to obtain a fast response. Intuitively, we expect the performance of a cascade control system to be superior (generally) to a standard single-input single-output (SISO) feedback control system (as long as there are no measurement lags on the states), since more system information (outputs) is being fed-back to the control system.

Input/output (transfer function) analysis is often used to design feedback control systems for chemical processes. Cascade control systems are usually designed by first tuning a slave control loop based on the transfer function model of the secondary process. If the slave loop can be tuned "fast" enough, then the master loop can be tuned based on the primary process transfer function, independent of the slave loop. If the bandwidth of the slave loop is close to that of the primary loop, then the loops must be iteratively tuned, until acceptable performance of the entire closed-loop process is obtained. Implicit in the typical controller design process is the assumption that the secondary and primary processes are decoupled. This is illustrated by the typical series cascade control block diagram, shown in Figure 2. The output of the secondary process is the input to the primary process in a series cascade control block diagram. Similarly, a parallel cascade control structure (in which the manipulated input has a direct effect on both of the outputs) is shown in Figure 3.

The objective of this paper is to show that an input/output representation of a cascade control system may not capture the true behavior of the closed-loop system

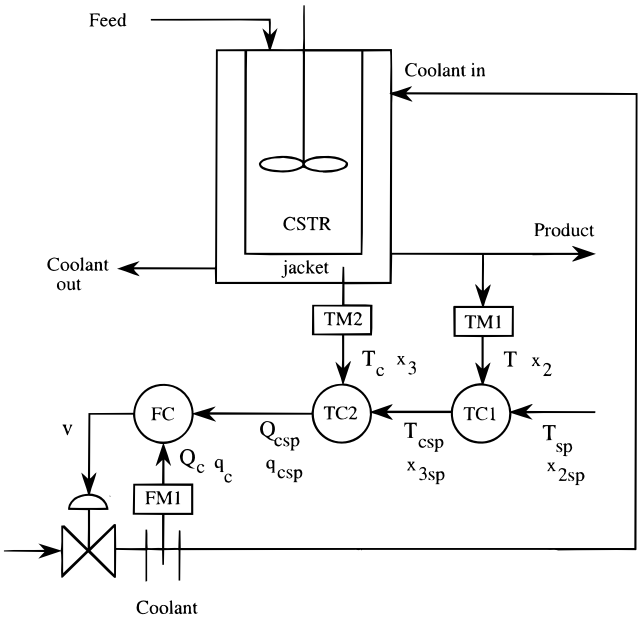

Figure 1. Process flow diagram (showing the control loops) for cascade control of reactor temperature in a CSTR.

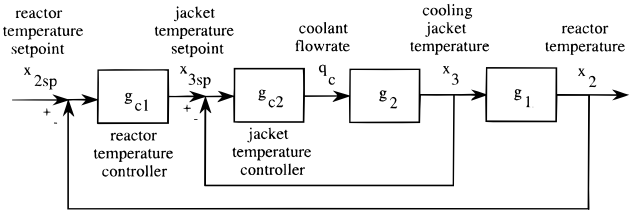

Figure 2. Series cascade control structure for a CSTR.

if the primary and secondary processes are coupled through the state-space model. The motivating problem is cascade control of an exothermic continuous-stirred-tank reactor (CSTR). Although many new nonlinear control techniques have been developed (Bequette, 1991; McLellan et al., 1990; Kravaris and Kantor, 1990), we use linear control for two reasons: (1) Linear feedback and cascade controllers are still the dominant strategies used in industry. (2) The linear techniques are well-known and easy to use for comparison purposes.

1.2. CSTR Modeling Equations. The standard two-state CSTR model (Uppal et al., 1974) describing an exothermic diabatic irreversible first-order reaction

* To whom all correspondence should be addressed. Telephone: (518)276-6683. Fax: (518)276-4030. Email: bequeb@rpi.edu.

[†] Present address: Exxon Chemicals, Baytown, TX.

S0888-5885(96)00677-X CCC: $14.00

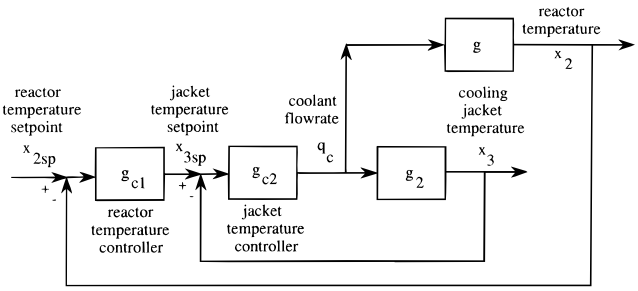

Figure 3. Parallel cascade control structure for a CSTR.

(A → B) is a set of two nonlinear ordinary differential equations obtained from dynamic material and energy balances (with the assumptions of constant volume, perfect mixing, negligible cooling-jacket dynamics, and constant physical parameters).

$$\frac{dC_a}{dt} = \frac{Q}{V}(C_{af} - C_a) - k_0 \exp\left(\frac{-E_a}{RT}\right)C_a \quad (1)$$

$$\frac{dT}{dt} = \frac{Q}{V}(T_f - T) - \frac{UA}{V\rho C_p}(T - T_c) + \left(\frac{-\Delta H}{\rho C_p}\right)k_0 \exp\left(\frac{-E_a}{RT}\right)C_a \quad (2)$$

where C_a and T are the concentration of component A and the temperature in the reactor, respectively. An additional energy balance around the cooling jacket assuming perfect mixing yields

$$\frac{dT_c}{dt} = \frac{Q_c}{V_c}(T_{cf} - T_c) + \frac{UA}{V_c\rho_c C_{pc}}(T - T_c) \quad (3)$$

where T_c is the cooling-jacket temperature. Equations 1−3 can be written in dimensionless form as

$$\frac{dx_1}{d\tau} = q(x_{1f} - x_1) - \phi x_1 \kappa(x_2) \quad (4)$$

$$\frac{dx_2}{d\tau} = q(x_{2f} - x_2) - \delta(x_2 - x_3) + \beta\phi x_1 \kappa(x_2) \quad (5)$$

$$\frac{dx_3}{d\tau} = \delta_1[q_c(x_{3f} - x_3) + \delta\delta_2(x_2 - x_3)] \quad (6)$$

where x_1, x_2, x_3, and q_c are the dimensionless concentration, reactor temperature, cooling-jacket temperature, and cooling-jacket flowrate, respectively. The dimensionless cooling-jacket flowrate q_c is the manipulated input, while the dimensionless reactor temperature x_2 and dimensionless cooling-jacket temperature x_3 are the measured outputs. The dimensionless variables and parameters (for example, ϕ, q, β, etc.) are defined in Table 1. Representative values of the parameters are listed in Table 2. Case 1 is open-loop stable over the entire region of operation for the two-state CSTR model (cf. Figure 4) but open-loop unstable in a certain operating region for the three-state CSTR model (cf. Figure 5). Case 2 exhibits ignition/extinction behavior for the two- (cf. Figure 6) and three-state models (cf. Figure 7). It is well-known (Uppal et al., 1974) that the exponential relationship of reaction rate with respect to reactor temperature is one of the major nonlinearities of the CSTR. We studied the steady-state nonlinearities (output and input multiplicities, infeasible operation regions) and the dynamic nonlinearities (quasiperiodic bifurcation behavior) of the three-state CSTR model in Russo and Bequette (1995, 1996).

Often it is assumed that the inner-loop controller can be tightly (perfectly) tuned, so that only the outer-loop tuning is considered. This assumption has usually been made in CSTR control and is why the two-state model is generally used. The steady-state input/output behavior of this CSTR, shown in Figures 4 and 5 for case 1 conditions, illustrates why one must be careful when using the classical two-state model (which assumes perfect inner-loop control) in the controller design. The

Table 1. Dimensionless Variables and Parameters for the Two- and Three-State CSTR Models

$x_1 = C_a/C_{afo}$	$x_2 = \dfrac{T - T_{fo}}{T_{fo}}\gamma$	$x_3 = \dfrac{T_c - T_{fo}}{T_{fo}}\gamma$
$q_c = Q_c/Q_o$	$\gamma = E_a/RT_{fo}$	$\kappa(x_2) = \exp\left(\dfrac{x_2}{1 + x_2/\gamma}\right)$
$\beta = \dfrac{(-\Delta H)C_{afo}}{\rho C_p T_{fo}}\gamma$	$\delta = UA/\rho C_p Q_o$	$\phi = (V/Q_o)k_o e^{-\gamma}$
$q = Q/Q_o$	$\tau = (Q_o/V)t$	$\delta_1 = V/V_c$
$\delta_2 = \rho C_p/\rho_c C_{pc}$	$x_{1f} = C_{af}/C_{afo}$	$x_{2f} = \dfrac{T_f - T_{fo}}{T_{fo}}\gamma$
$x_{3f} = \dfrac{T_{cf} - T_{fo}}{T_{fo}}\gamma$		

Table 2. Two- and Three-State CSTR Model Parameter Values

parameter	case 1	case 2	parameter	case 1	case 2
ϕ	0.11	0.072	δ_1	10	10
β	7.0	8.0	δ_2	1.0	1.0
δ	0.5	0.3	x_{1f}	1.0	1.0
γ	20	20	x_{2f}	0.0	0.0
q	1.0	1.0	x_{3f}	−1.0	−1.0

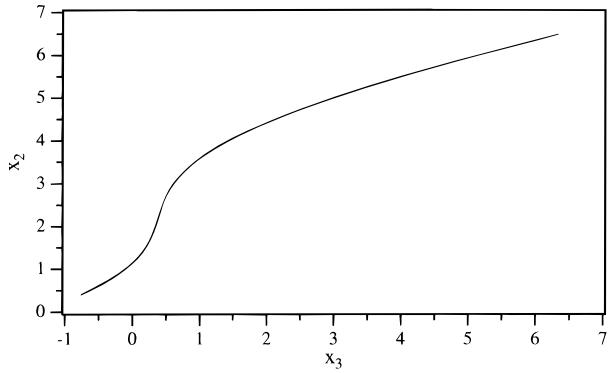

Figure 4. Steady-state dimensionless reactor temperature versus cooling-jacket temperature for the jacketed exothermic CSTR, case 1 conditions.

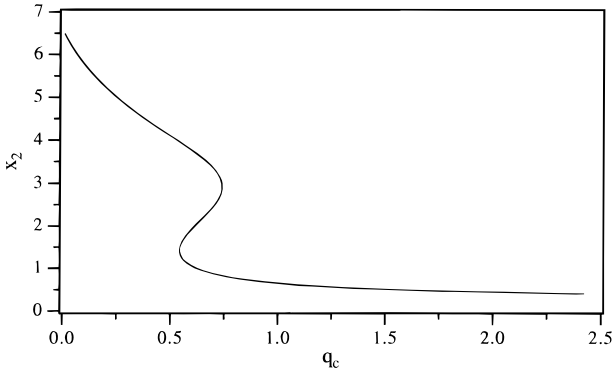

Figure 5. Steady-state dimensionless reactor temperature versus cooling-jacket flowrate for the jacketed exothermic CSTR, case 1 conditions.

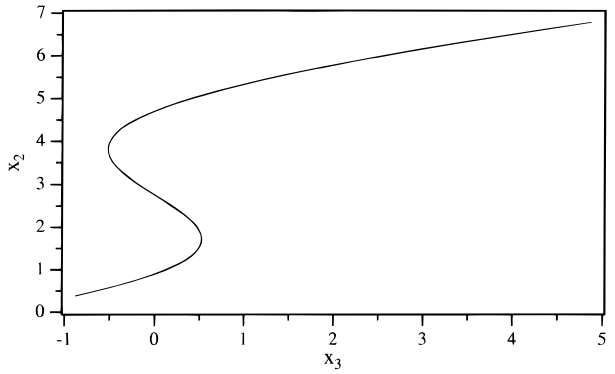

Figure 6. Steady-state dimensionless reactor temperature versus cooling-jacket temperature for the jacketed exothermic CSTR, case 2 conditions.

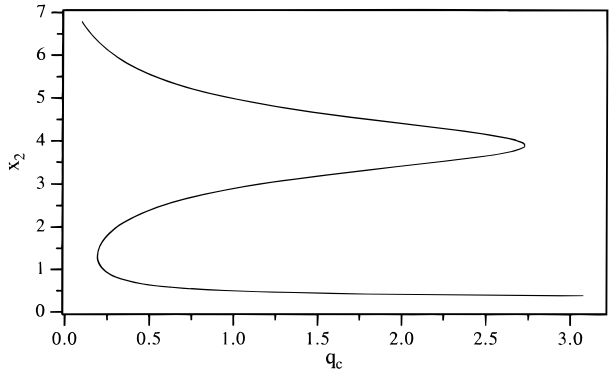

Figure 7. Steady-state dimensionless reactor temperature versus cooling-jacket flowrate for the jacketed exothermic CSTR, case 2 conditions.

Table 3. Definitions of the Transfer Function Polynomials for the CSTR Models

$$g(s) = \delta\delta_1(x_{3f} - x_{3s})\frac{s + C_1}{s^3 + A_1s^2 + A_2s + A_3} = k\frac{c_1s + 1}{a_3s^3 + a_2s^2 + a_1s + 1}$$

$$g_1(s) = \delta\frac{s + C_1}{s^2 + B_1s + B_2} = k_1\frac{c_1s + 1}{b_2s^3 + b_1s^2 + 1}$$

$$g_2(s) = \delta_1(x_{3f} - x_{3s})\frac{s^2 + B_1s + B_2}{s^3 + A_1s^2 + A^2s + A_3} = k_2\frac{b_2s^2 + b_1s + 1}{a_3s^3 + a_2s^2 + a_1s + 1}$$

relationship between jacket temperature and reactor temperature, shown in Figure 4, has monotonic input/output behavior and indicates that the system is open-loop stable over the entire region. Contrast this with the relationship between jacket flowrate and reactor temperature, shown in Figure 5, which indicates hysteresis behavior where the system is open-loop unstable over a significant range. If the CSTR is being operated at an open-loop unstable operation point (say, $x_2 = 2.0$) and the cooling jacket flowrate hits a constraint (thus effectively "opening up" the control loop), then the two-state model incorrectly predicts stable behavior (cf. Figure 4) while the three-state model will correctly predict instability. Systems with this type of steady-state input/output curve (e.g., Figure 5) are unstable (at least) over the range of reactor temperatures bounded by the limit points ($x_2 \approx 1.5-3.0$ in this example). The limit points are a bifurcation point where the linearized system has an eigenvalue at zero. Therefore, "inside" the limit points the linearized system has an eigenvalue with a positive real part, indicating instability.

Table 4. Transfer Function Coefficients

$c_1 = 1/C_1$	$b_1 = B_1/B_2$	$b_2 = 1/B_2$
$a_1 = A_2/A_3$	$a_2 = A_1/A_3$	$a_3 = 1/A_3$

Table 5. Definitions of the Transfer Function Gains for the CSTR Models

$$k = \delta\delta_1(x_{3f} - x_{3s})\frac{C_1}{A_3} \qquad k_2 = \delta_1(x_{3f} - x_{3s})\frac{B_2}{A_3} \qquad k_1 = \delta\frac{C_1}{A_3}$$

Table 6. Definitions of C_1–A_3 in Terms of the CSTR Parameters

$$C_1 = \frac{qx_{1f}}{x_{1s}}$$

$$B_1 = \frac{qx_{1f}}{x_{1s}} + (q + \delta) - \beta q\frac{x_{1f} - x_{1s}}{\left(1 + \frac{x_{2s}}{\gamma}\right)^2}$$

$$B_2 = \frac{(q + \delta)qx_{1f}}{x_{1s}} - \beta q^2\frac{(x_{1f} - x_{1s})}{\left(1 + \frac{x_{2s}}{\gamma}\right)^2}$$

$$A_1 = B_1 + \delta_1(\delta\delta_2 + q_{cs})$$

$$A_2 = B_2 + \delta_1[(\delta\delta_2 + q_{cs})B_1 - \delta^2\delta_2]$$

$$A_3 = \delta_1\left[(\delta\delta_2 + q_{cs})B_2 - \frac{\delta^2\delta_2 qx_{1f}}{x_{1s}}\right]$$

2. Cascade Control Structure

2.1. Transfer Function Models. The transfer functions between the deviation variables $x_2'(s)$, $x_3'(s)$, and $q_c'(s)$ are

$$x_2'(s) = g(s)\, q_c'(s)$$

$$= k\frac{c_1s + 1}{a_3s^3 + a_2s^2 + a_1s + 1}q_c'(s) \tag{7}$$

$$x_2'(s) = g_1(s)\, x_3'(s)$$

$$= k_1\frac{c_1s + 1}{b_2s^2 + b_1s + 1}x_3'(s) \tag{8}$$

$$x_3'(s) = g_2(s)\, q_c'(s)$$

$$= k_2\frac{b_2s^2 + b_1s + 1}{a_3s^3 + a_2s^2 + a_1s + 1}q_c'(s) \tag{9}$$

where the gains and coefficients of the transfer functions are given in Tables 3–6 (the prime indicates a deviation variable). We can view these equations in block diagram form, as shown in Figure 8.

The poles of the two-state model relationship (relating $x_2'(s)$ to $x_3'(s)$), $g_1(s)$, are the zeros of the $x_3'(s)$–$q_c'(s)$ relationship in the three-state model, $g_2(s)$. When $g_1(s)$ is unstable at a particular operating point, then $g_2(s)$ will have right-half-plane zeros. We would think that the performance of the "inner-loop" process would be reduced, since right-half-plane zeros cannot be "inverted" for "perfect" control. We find that this is not the case, because the real cascade system is actually a multiple-state feedback control. Since the real controller measures two outputs and manipulates a single

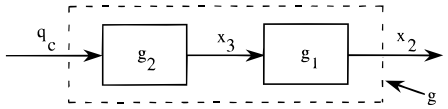

Figure 8. Relationship between the open-loop transfer functions.

input, there are no problems with the secondary process right-half-plane zeros.

2.2. Series and Parallel Cascade Control. The two most typical cascade control configurations are the series and parallel structures, which were shown in Figures 2 and 3. Luyben (1973) stressed the differences between conventional series cascade control and parallel cascade control. The three-state CSTR transfer function models have a parallel cascade control structure, since the manipulated variable q_c (dimensionless cooling-jacket flowrate) has a direct influence on x_2 (dimensionless reactor temperature) and x_3 (dimensionless cooling-jacket temperature) through parallel transfer functions.

In this section we show that the traditional methods of analyzing cascade control (based on series or parallel input/output relationships) should not be used when the primary and secondary processes are coupled, and the process is open-loop unstable. Consider the series cascade control case, shown in Figure 2. The state-space realization is

$$A_{\text{series}} = \begin{pmatrix} a_{11} & a_{12} & 0 & 0 & 0 \\ a_{21} & a_{22} & a_{23} & 0 & 0 \\ 0 & a_{32} & a_{33} & 0 & 0 \\ 0 & 0 & 0 & a_{11} & a_{12} \\ 0 & 0 & a_{23} & a_{21} & a_{22} \end{pmatrix}$$

$$B_{\text{series}} = \begin{pmatrix} 0 \\ 0 \\ b_{31} \\ 0 \\ 0 \end{pmatrix}$$

$$C_{\text{series}} = \begin{pmatrix} 0 & 0 & 1 & 0 & 0 \\ 0 & 0 & 0 & 0 & 1 \end{pmatrix}$$

where states 1−3 represent the secondary process and states 4 and 5 represent the primary process transfer functions, respectively. The coefficients of the A_{series} and B_{series} matrices come from the original open-loop **A** and **B** matrices for the three-state CSTR model. The first ($C_{\text{series13}} = 1$) and second outputs ($C_{\text{series25}} = 1$) correspond to the dimensionless cooling-jacket and reactor temperatures, respectively.

One can do a simple calculation of the controllability matrix (Kailath, 1980) and show that it is not full rank. Hence, the state-space realization of the two open-loop transfer functions in series results in a state-space model with a nonminimal realization, because the primary and secondary processes are actually coupled. The controllable subsystem, obtained from a decomposition of the system into uncontrollable and controllable modes (Kailath, 1980), has the same transfer function as the original system. In our case the controllable subsystem is simply the three-state model due to the series structure. The three-state model is itself controllable and observable, making it a minimal realization. The uncontrollable subsystem is the two-state model. Therefore, when the secondary and primary processes are unstable, the uncontrollable modes are unstable, which results in the system not being stabilizable (Kailath, 1980).

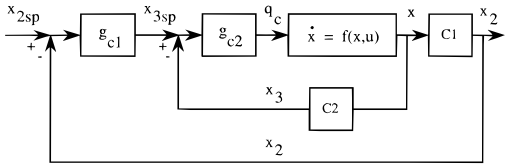

Figure 9. Coupled process formulation using a state-space representation. The controller design is based on a linear state-space model. Actual implementation is on a nonlinear process.

Consider the case of parallel cascade control (Figure 3) of the jacketed exothermic CSTR. The state-space realization is

$$A_{\text{parallel}} = \begin{pmatrix} a_{11} & a_{12} & 0 & 0 & 0 & 0 \\ a_{21} & a_{22} & a_{23} & 0 & 0 & 0 \\ 0 & a_{32} & a_{33} & 0 & 0 & 0 \\ 0 & 0 & 0 & a_{11} & a_{12} & 0 \\ 0 & 0 & 0 & a_{21} & a_{22} & a_{23} \\ 0 & 0 & 0 & 0 & a_{32} & a_{33} \end{pmatrix}$$

$$B_{\text{parallel}} = \begin{pmatrix} 0 \\ 0 \\ b_{31} \\ 0 \\ 0 \\ b_{31} \end{pmatrix}$$

$$C_{\text{parallel}} = \begin{pmatrix} 0 & 0 & 1 & 0 & 0 & 0 \\ 0 & 0 & 0 & 0 & 1 & 0 \end{pmatrix}$$

where states 1−3 represent the secondary process and states 4−6 represent the primary process transfer functions, respectively. The coefficients of the A_{parallel} and B_{parallel} matrices come from the original open-loop **A** and **B** matrices. The first ($C_{\text{parallel13}} = 1$) and second outputs ($C_{\text{parallel25}} = 1$) correspond to the dimensionless cooling-jacket and reactor temperatures, respectively.

Once again, a calculation of the controllability matrix (Kailath, 1980) shows that it is not full rank; therefore, the state-space realization of the two open-loop transfer functions in parallel results in a state-space model with a nonminimal realization. As before, the controllable subsystem has the same transfer function as the original system. When the primary process is unstable, the uncontrollable modes are also unstable, since the two subsystems are equivalent in the parallel case. Therefore, the system is not stabilizable (Kailath, 1980). This configuration suffers from internal stability problems when the primary and secondary processes are unstable. Hence, the unstable modes cannot be stabilized and a process so-simulated will be unstable, while the actual process may be stable.

If the parallel or series representation is used to simulate the closed-loop behavior of an open-loop unstable system, simulation may predict instability when the physical system is stable. It is important then, in block diagram programming environments (SIMULINK, for example), to use a minimal state-space representation of the process. The actual coupled process is best represented by Figure 9, where it is shown clearly that the primary and secondary outputs are coupled through the process model.

3. Control System Design

3.1. Cascade Control System Design. In section 2.2 we saw that traditional methods of analyzing

cascade control (based on series and parallel input/output relationships) should not be used when the primary and secondary processes are coupled, and the process is open-loop unstable. Parallel or series representations may predict (incorrectly) that the closed-loop behavior will be unstable. However, using a full state-space model in the control system design procedure captures the coupled nature of the process dynamics. Since cascade controllers are often directly implemented in industry without using simulation for controller design and testing, problems with the input/output formulation have not been observed as frequently as they actually occur.

Let us consider the ubiquitous case when a PI/P controller structure is used for the outer and inner loops, respectively. Integral action in the outer loop can be attained by appending an additional state variable to the model:

$$\dot{x}_4 = x_2 \tag{10}$$

The state feedback controller is given by

$$u = -\mathbf{K}x \tag{11}$$

where the feedback gain row vector is

$$\mathbf{K} = \begin{bmatrix} 0 & k_{c2}k_{c1} & k_{c2} & \dfrac{k_{c2}k_{c1}}{\tau_{I1}} \end{bmatrix} \tag{12}$$

As one can see, cascade control can be thought of as partial state feedback. Note that the first feedback gain is constrained to be zero with this controller structure (because we are assuming that the first state cannot be measured or reconstructed with an observer). Hence, arbitrary relocation of the "closed-loop" poles is not possible. One potential problem with this type of design procedure is that a stabilizing feedback gain (**K**) may not exist; i.e., the constrained controller structure may not, in general, be able to stabilize the process. In some industrial applications the control structure is limited to P, PI, or PID.

3.2. IMC-Based Control System Design. Internal model control (IMC) (Morari and Zafiriou, 1989) provides a clear framework for controller design. One advantage to the IMC procedure is that it simplifies controller tuning because a single tuning parameter, λ, is used as opposed to the three parameters (k_c, τ_I, τ_D) for a PID controller. Linear controllers are often not valid over a wide range of operating regions due to process nonlinearities. However, since we are concerned here with operation in a small region where the stability characteristics do not change, linear controllers generally provide acceptable performance.

It is well-known that for open-loop unstable responses, the IMC controller must be implemented in conventional feedback form since the IMC form is internally unstable (Morari and Zafiriou, 1989).

$$g_c(s) = \frac{q(s)}{1 - \tilde{g}(s)\, q(s)} \tag{13}$$

Here $g_c(s)$ and $\tilde{g}(s)$ are the feedback controller and process model transfer functions, while $q(s)$ is the IMC controller. The IMC controller is

$$q(s) = \tilde{g}_-^{-1}(s)\, f(s) \tag{14}$$

where $\tilde{g}_-^{-1}(s)$ is the invertible part of the process transfer function and $f(s)$ is a filter transfer function which is added to make the IMC controller proper. Rivera et al. (1986) demonstrate that for a large number of single-input single-output (SISO) linear systems the IMC design procedure yields PID-type controllers. There are many possible choices for the IMC filter structure; one possible structure for open-loop unstable systems is

$$f(s) = \frac{e_k s^k + e_{k-1}s^{k-1} + \ldots + e_1 s + e_0}{(\lambda s + 1)^n} \tag{15}$$

Here k is the number of distinct poles in the right-half-plane (RHP), n is chosen to make the IMC controller $q(s)$ proper, and λ is the filter time constant. The IMC filter is chosen such that its steady-state gain is unity; for open-loop unstable systems, the filter must also be unity at the k unstable poles (Morari and Zafiriou, 1989)

$$f(s) = 1 \qquad \text{at} \quad s = p_i \tag{16}$$

where p_i is the ith unstable pole of $g(s)$. Rotstein and Lewin (1991) showed that the IMC design procedure for some first- and second-order unstable transfer functions (without numerator dynamics) results in PID feedback controllers. The choice of the IMC filter $f(s)$ and subsequently controller structure for the inner and outer loops of the cascade control scheme depends on the number of right-half-plane (RHP) zeros and poles.

3.3. IMC-Based Design for Cascade Control. In this section an IMC-based feedback control system design procedure is developed for cascade control of reactor temperature. The cascade control system design procedure is based on IMC-based feedback control of the "outer-loop" process, assuming a controller (proportional control, for example) has been designed for the inner-loop process. The inner-loop controller then is explicitly accounted for in the design of the outer-loop controller.

In order to develop the controller design procedure, we linearize the three-state CSTR model to obtain the following state-space model:

$$\dot{\mathbf{x}} = \mathbf{A}\mathbf{x} + \mathbf{B}u \tag{17}$$

$$y = \mathbf{C}\mathbf{x} \tag{18}$$

where $u = q_c'(t)$, the dimensionless coolant flowrate. We assume a proportional controller k_{c2} has been designed for the inner loop:

$$q_c'(t) = k_{c2}(x_3(t) - x_{3sp}(t)) \tag{19}$$

Therefore, the state-space model that we use to design the outer-loop controller becomes

$$\dot{\mathbf{x}} = \bar{\mathbf{A}}\mathbf{x} + \bar{\mathbf{B}}x_{3sp} \tag{20}$$

$$y = \bar{\mathbf{C}}\mathbf{x} \tag{21}$$

where $\bar{\mathbf{A}}$, $\bar{\mathbf{B}}$, and $\bar{\mathbf{C}}$ are given by

$$\bar{\mathbf{A}} = \mathbf{A} - [\mathbf{0} \quad \ldots \quad \mathbf{0} \quad \bar{\mathbf{B}}] \tag{22}$$

$$\bar{\mathbf{B}} = \mathbf{B}k_{c2} \tag{23}$$

$$\bar{\mathbf{C}} = [0 \quad 1 \quad 0] \tag{24}$$

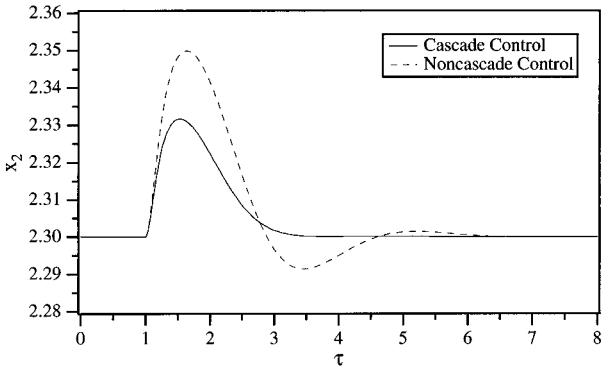

Figure 10. Comparison of the closed-loop dimensionless reactor temperature performance of the cascade and standard SISO feedback control strategies to a disturbance in the cooling-jacket feed temperature.

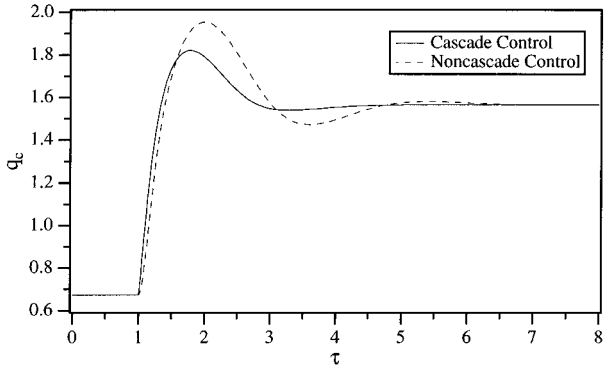

Figure 11. Comparison of the closed-loop dimensionless cooling-jacket flowrate performance of the cascade and standard SISO feedback control strategies to a disturbance in the cooling-jacket feed temperature.

The transfer function used in the controller design is

$$y(s) = \bar{\mathbf{C}}(s\mathbf{I} - \bar{\mathbf{A}})^{-1}\bar{\mathbf{B}}x_{3\mathrm{sp}}(s)$$
$$= \bar{g}(s)\, x_{3\mathrm{sp}}(s) \qquad (25)$$

The IMC design procedure can be used on $\bar{g}(s)$, which in our case turns out to be minimum phase and is of the following form:

$$\bar{g}(s) = \bar{k}\,\frac{\tau_n s + 1}{(\tau_1 s + 1)(\tau_2 s + 1)(-\tau_u s + 1)} \qquad (26)$$

The achievable closed-loop response, assuming that the linear model captures the entire behavior of the process (e.g., perfect linear model), is given by

$$x_2(s) = \frac{\theta s + 1}{(\lambda s + 1)^3} x_{2\mathrm{sp}}(s) \qquad (27)$$

where θ is chosen to satisfy the IMC filter $f(s)$ unity gain condition at the unstable pole.

4. Control Case Studies

The IMC-based feedback cascade controller is obtained using eq 25 with eqs 13 and 15. The resulting outer-loop controller is a PI with a double lead-lag. Generally, one of the poles of this controller is fast, hence, a reduced-order PI with a lead-lag controller can be used with very little performance degradation. We compare the robustness of standard feedback (SISO) and cascade feedback (SIMO) control with our new cascade design procedure, applied to the nonlinear process. The inner-loop proportional gain is $k_{c2} = -0.5$, and the IMC filter time constant is $\lambda = 0.2$ for both sets of simulations.

The first case study deals with the effect of an unmeasured disturbance on the performance of cascade feedback (SIMO) and standard feedback (SISO) controllers. The reactor parameters are case 1 conditions; the nominal setpoint is $x_2 = 2.3$ (which is open-loop unstable). The linearized open-loop **A** and **B** matrices at $x_2 = 2.3$ for case 1 conditions are given in the Appendix. An unmeasured disturbance in the dimensionless cooling-jacket feed temperature ($x_{3\mathrm{f}}$) occurs at $\tau = 1$ ($x_{3\mathrm{f}}$ changes from -1 to -0.2). Figures 10 and 11 demonstrate that the cascade control scheme does a better job of rejecting the unmeasured disturbance in the dimensionless cooling-jacket feed temperature. An interesting point is that, if we had analyzed a two-state CSTR model (neglecting cooling-jacket dynamics), one would think that it would be possible to arbitrarily detune the system, because case 1 is open-loop stable for the two-state CSTR model.

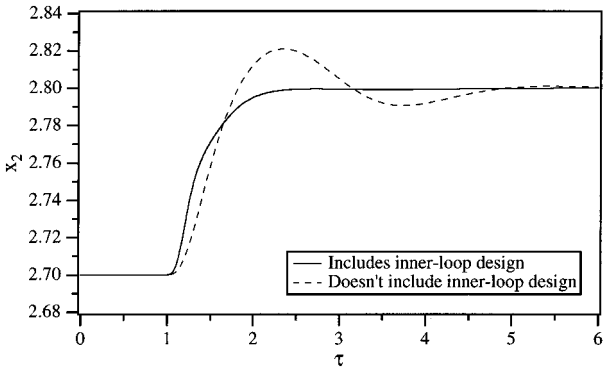

Figure 12. Comparison of the closed-loop dimensionless reactor temperature performance of the two cascade control strategies.

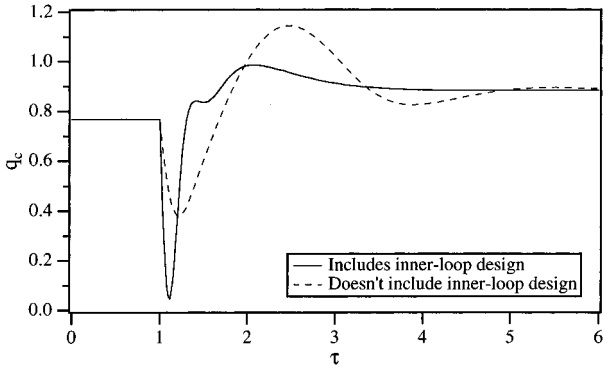

Figure 13. Comparison of the closed-loop dimensionless cooling-jacket flowrate performance of the two cascade control strategies.

The second case study considers the influence of the cascade control system design. The reactor parameters are case 2 conditions; the nominal setpoint is $x_2 = 2.7$ (which is open-loop unstable). The linearized open-loop **A** and **B** matrices at $x_2 = 2.7$ for case 2 conditions are given in the Appendix. A setpoint filter ($\tau_F = 0.45 \approx 2\lambda$) is used to remove the overshoot which results from the ISE-optimal IMC design procedure. The setpoint of the dimensionless temperature (x_2) is changed from 2.7 to 2.8 at $\tau = 1$. Figures 12 and 13 demonstrate that our cascade design procedure is superior to the normal cascade control design where the inner-loop controller design is not incorporated in the outer-loop design.

5. Conclusions

We have shown in this work that traditional methods of analyzing cascade control should not be used when the primary and secondary processes are coupled (through the state-space model) and the process is open-loop unstable. The parallels between traditional full-state feedback control and cascade control were demonstrated. A jacketed CSTR example was used to show that neither the parallel nor series input/output formulation for cascade control satisfies controllability or stabilizability conditions when the process is open-loop unstable, although these conditions are satisfied by the physical (state-space) model. The cascade control system design procedure developed in this paper was limited to linear control structures where an inner-loop controller gain has been prespecified. This control system design could be extended to nonlinear systems using a GLC-type of approach (Kravaris and Kantor, 1990).

Acknowledgment is made to the donors of the the Petroleum Research Fund, administered by the American Chemical Society. A portion of this work was performed while B.W.B. was on sabbatical at Northwestern University.

Nomenclature

A = heat-transfer area
$A_{parallel}$ = state-space **A** matrix for the parallel cascade state-space realization
A_{series} = state-space **A** matrix for the series cascade state-space realization
$B_{parallel}$ = state-space **B** matrix for the parallel cascade state-space realization
B_{series} = state-space **B** matrix for the series cascade state-space realization
$C_{parallel}$ = state-space **C** matrix for the parallel cascade state-space realization
C_{series} = state-space **C** matrix for the series cascade state-space realization
C_a = concentration of reactant A in the reactor
C_{af} = concentration of reactant A in the reactor feed
C_p = heat capacity of the feed and products
C_{pc} = heat capacity of the jacket fluid
E_a = activation energy in Arrhenius reaction rate
$g(s)$ = transfer function relating $x_2'(s)$ and $q_c'(s)$
$g_1(s)$ = transfer function relating $x_2'(s)$ and $x_3'(s)$
$g_2(s)$ = transfer function relating $x_3'(s)$ and $q_c'(s)$
ΔH = heat of reaction
K = state feedback controller gain row vector
k_{c1} = inner-loop proportional gain
k_{c2} = outer-loop proportional gain
k_0 = preexponential factor in Arrhenius reaction rate
q = dimensionless reactor flow rate
Q = reactor flowrate
$q(s)$ = IMC controller transfer function
q_c = dimensionless cooling-jacket flowrate
Q_c = cooling-jacket flowrate
R = universal gas content
t = time
s = Laplace transform variable
T = reactor temperature
T_c = cooling-jacket temperature
T_{cf} = cooling-jacket feed temperature
T_f = reactor feed temperature
u = state feedback controller manipulated input
U = overall heat-transfer coefficient
V = reactor volume
V_c = cooling-jacket volume
x = vector of system states
x_1 = dimensionless reactor concentration
x_{1f} = dimensionless reactor feed concentration
x_2 = dimensionless reactor feed temperature
x_{2f} = dimensionless reactor feed temperature
x_3 = dimensionless cooling-jacket temperature
x_{3f} = dimensionless cooling-jacket feed temperature

Greek Symbols

β = dimensionless heat of reaction
γ = dimensionless activation energy
δ = dimensionless heat-transfer coefficient
δ_1 = reactor to cooling-jacket volume ratio
δ_2 = reactor to cooling-jacket density heat capacity ratio
$\kappa(x_2)$ = dimensionless Arrhenius reaction rate nonlinearity
λ = IMC filter time constant
ρ = density of the feed and products
ρ_c = density of the jacket fluid
τ = dimensionless time
τ_{I1} = outer-loop integral time constant
ϕ = nominal Damkohler number based on the reactor feed

Appendix. A and B Matrices for the Three-State CSTR Model

The **A** and **B** matrices for the first case study (obtained by linearizing the three-state CSTR model at $x_2 = 2.3$ for case 1 conditions) are

$$\mathbf{A} = \begin{bmatrix} -1.8655 & -0.3732 & 0.0 \\ 6.0582 & 1.1122 & 0.5 \\ 0.0 & 5.0 & -11.7450 \end{bmatrix}$$

$$\mathbf{B} = \begin{bmatrix} 0.0 \\ 0.0 \\ -14.0485 \end{bmatrix}$$

The **A** and **B** matrices for the second case study (obtained by linearizing the three-state CSTR model at $x_2 = 2.7$ for case 2 conditions) are

$$\mathbf{A} = \begin{bmatrix} -1.7771 & -0.3394 & 0.0 \\ 6.2165 & 1.4155 & 0.3 \\ 0.0 & 3.0 & -10.6795 \end{bmatrix}$$

$$\mathbf{B} = \begin{bmatrix} 0.0 \\ 0.0 \\ -10.3937 \end{bmatrix}$$

Literature Cited

Bequette, B. W. Nonlinear Control of Chemical Processes: A Review. *Ind. Eng. Chem. Res.* **1991**, *30*, 1391.
Kailath, T. *Linear Systems*; Prentice Hall: Englewood Cliffs, NJ, 1980.
Kravaris, C.; Kantor, J. C. Geometric Methods for Nonlinear Process Control. 1−2. *Ind. Eng. Chem. Res.* **1990**, *29*, 2295.
Luyben, W. L. Parallel Cascade Control. *Ind. Eng. Chem. Fundam.* **1973**, *12*, 463.
McLellan, P. J.; Harris, T. J.; Bacon, D. W. Error Trajectory Descriptions of Nonlinear Controller Designs. *Chem. Eng. Sci.* **1990**, *45*, 3017.
Morari, M.; Zafiriou, E. *Robust Process Control*; Prentice Hall: Englewood Cliffs, NJ, 1989.
Rivera, D. E.; Morari, M.; Skogestad, S. Internal Model Control. 4. PID Controller Design. *Ind. Eng. Chem. Process Des. Dev.* **1986**, *25*, 252.
Rotstein, G. E.; Lewin, D. R. Simple PI and PID Tuning for Open-loop Unstable Systems. *Ind. Eng. Chem. Res.* **1991**, *30*, 1864.

Russo, L. P.; Bequette, B. W. Impact of Process Design on the Multiplicity Behavior of a Jacketed Exothermic CSTR. *AIChE J.* **1995**, *41*, 135.

Russo, L. P.; Bequette, B. W. Effect of Process Design on the Open-loop Behavior of a Jacketed Exothermic CSTR. *Comput. Chem. Eng.* **1996**, *20*, 417.

Uppal, A.; Ray, W. H.; Poore, A. B. On the Dynamic Behavior of Continuous Stirred Tank Reactors. *Chem. Eng. Sci.* **1974**, *29*, 967.

Received for review October 21, 1996
Revised manuscript received March 10, 1997
Accepted March 11, 1997[⊗]

IE960677O

[⊗] Abstract published in *Advance ACS Abstracts,* May 1, 1997.